Influence of Sensor Design on Bio-Inspired, Adaptive Acoustic Sensing

Ekram Khan[1], Claudia Lenk[1], Andreas Männchen[2], Jan Küller[2], Daniel Beer[2], Vishal Gubbi[1], Tzvetan Ivanov[1], Martin Ziegler[1]

[1] *Dept. Micro- and nanoelectronic systems, Technische Universität Ilmenau, 98693 Ilmenau, Deutschland, Email: claudia.lenk@tu-ilmenau.de*

[2] *Fraunhofer Institute for Digital Media Technology, 98693 Ilmenau, Germany, Email: daniel.beer@idmt.fraunhofer.de*

Introduction

Intelligent sound processing systems are ubiquitous today. Be it the speech processing performed by voice assistants in smartphones and smart speakers or the acoustic monitoring conducted in industrial applications to ensure machine integrity or product quality—information is extracted from audio recordings in real time, seemingly everywhere, almost constantly.
Current sound processing systems usually perform three major steps (see, e.g., [1]), as schematically shown in Figure 1: *(1) Sound detection or transduction* using a microphone; *(2) signal conditioning and feature extraction* implemented with signal processing algorithms of varying complexity; and the actual *(3) sound processing*, such as classification, based on neural networks (NN). These steps are mostly conducted sequentially.
While the performance of sound processing systems has been steadily increasing over the years, some unsolved problems remain (see, e.g., [2]). These include bad performance at low signal-to-noise ratios (SNRs), considerable latency due to the often software-based or even cloud-based signal conditioning and sound processing, as well as the inability to learn the necessary models locally, since they are highly complex and require high computation power.

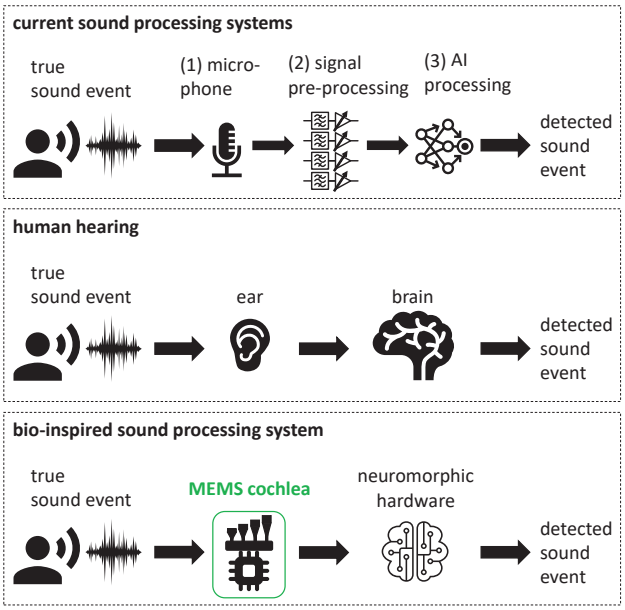

Figure 1: Comparison of sound processing systems and the human hearing process. While in current technological systems, signal processing and feature extraction take place after the transduction of the signal, these steps are performed before or during the transduction process in the mammalian ear and the bio-inspired MEMS cochlea.

We recently presented a novel bio-inspired acoustic sensor [3] that was designed in the hopes of tackling these problems by integrating the signal conditioning and feature extraction step into the transduction stage. In this sense, it is a microelectromechanical system (MEMS) inspired by the mammalian cochlea, leading to its name 'MEMS cochlea' (see Figure 1), consisting of one or more 'MEMS hair cells'. The MEMS hair cell is based on a linear acoustic transducer in connection with a high-speed feedback [3], which is used to tune the gain and linearity of the transducer's response to sound. Using the resonant mode for sensing and the dynamical tuning of transducer properties via the feedback, the sensor offers signal conditioning and feature extraction functionalities like bandpass filtering, frequency-selective amplification, adaptation to changing acoustic environments, and highlighting of sound onset or offset [3][4].

In this article, we focus on the influence of some important geometrical design parameters on the performance of MEMS hair cells as acoustic sensors. Thereby, changing the length and thickness of the silicon beam modifies the resonance frequency, i.e. the frequency filter property of the sensor [5]. Here, we study ways to improve the sensitivity without changing the resonance frequency. The study is based on FEM simulations and considers varying sensor geometries as well as different mountings. The simulation results are validated by comparing them to the results of measurements conducted with fabricated MEMS hair cells.

Basic Design and Simulations

The basic design of the transducer is shown in Figure 2. The transducer is a single-side clamped silicon beam with integrated deflection sensing using the piezoresistive effect and with an integrated actuator based on the bimorph effect (thermomechanical actuation principle) [6][7]. The transducer operates as a pressure gradient sensor. The beam is surrounded by a silicon membrane with the same thickness as the beam, but the two are separated by a small air gap. If the gap is smaller than the thermoviscous layer thickness, it acts like a sound barrier, i.e. as a reflective, sound soft boundary. So impinging sound waves have to travel around the complete system of sensor and membrane. Thus, the combination of beam and membrane will increase the pressure gradi-

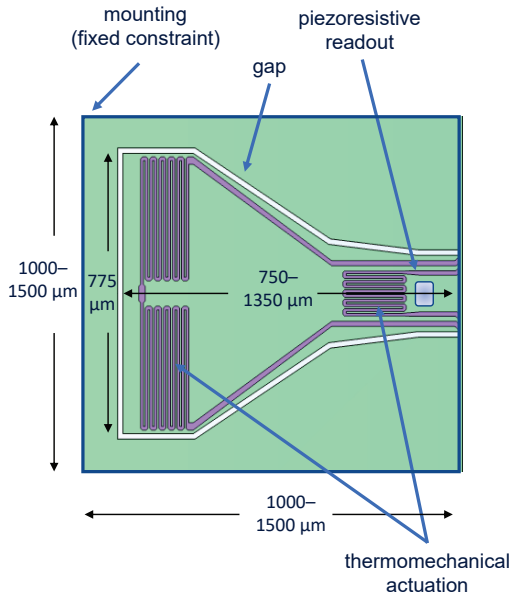

Figure 2: Technical drawing showing the basic transducer design layout, including the beam and a membrane surrounding it.

ent acting on the beam and, therefore, its sensitivity. We use 15 µm as standard gap size, thus the system behaves acoustically like one closed membrane for the whole auditory range.

Simulations were performed using COMSOL Multiphysics to verify the design concepts. For this study, the various topology changes (membrane area, gap size and mounting) were implemented in the model and the physical boundary conditions were realized with the pressure acoustics and structural mechanics module. The MEMS hair cell is excited by a plane wave with an amplitude of 1 Pa. Figure 3 shows the simulation setup.
Thermoviscous boundary layer effects are considered on all surfaces of the solid surrounded by air. They are approximated by using the thermoviscous boundary layer condition and narrow region acoustics in small gaps. The effects are known for sound propagation in or near small structures [8] and for oscillating microbeams in a gas or fluid environment [9]. If these effects are neglected, no valid results will be obtained. Additionally, for realistic deflection values, the mechanical damping must be considered. This was done using loss factor damping for each material; it is sufficiently accurate for the first eigenmode. The thermomechanical actuation is currently not considered, since only the linear passive behavior of the beam is important for the initial comparison of the design concepts.
The pressure difference between the front and back of the beam shown in Figure 3 causes the beam to oscillate, resulting in an electrical voltage due to the piezoresistive effect of the sensor. Since the sensing voltage linearly depends on the displacement at the free end of the beam (for a fixed beam geometry), the piezoresistive elements are not included in this study. Here, the maximum displacement at the free end of the beam is used as an indicator of the sensitivity.

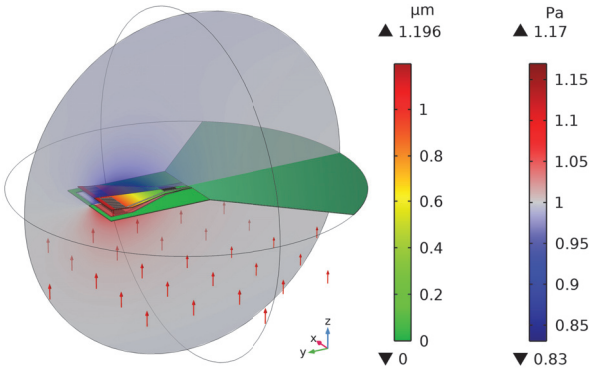

Figure 3: Sample setup for the simulation: The beam is mounted on one side (fixed constraint) and surrounded by a silicon membrane. The red arrows indicate the direction of the incoming plane wave excitation. The left color scale denotes the resulting displacement and the right color scale denotes the sound pressure.

Tuning the Sensitivity

As stated previously, the thermoviscous layer in the narrow gap between the beam and the membrane yields an acoustic coupling between both despite the lack of mechanical coupling. The thickness of the thermoviscous layers is strongly frequency-dependent: $d_{\mathrm{visc}} = \sqrt{2\mu/\omega\rho_{\mathrm{air}}}$ with the dynamic viscosity μ, the sound frequency ω and the density of air ρ_{air}. Thus, we study the effect of different gap sizes for fixed sound frequency and resonance frequency to analyze its effect on the sensitivity. As shown in Figure 4, increasing the gap size above 25 µm, yields a constant displacement of roughly 0.5 µm. Since the viscous boundary layer is approximately 28 µm (dashed red line in Figure 4) for the applied 4.5 kHz sound, the membrane and the beam are effectively decoupled for these gap sizes. In contrast, for smaller gap sizes, both are coupled and the displacement increases for decreasing gap sizes. Thus, the gap size can be used to tune the acoustic coupling strength between membrane and beam.

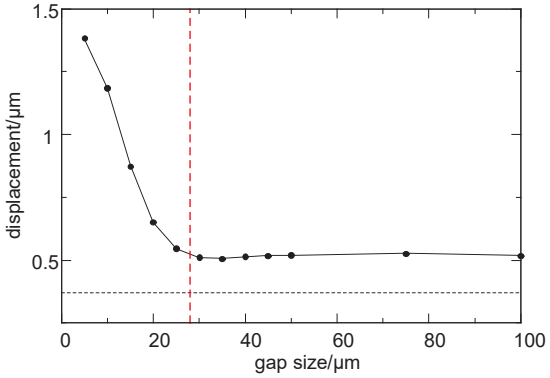

Figure 4: Maximal beam displacement as a function of the gap size between beam and membrane. The dashed red line indicates the thickness of the viscous boundary layer at the resonance frequency.

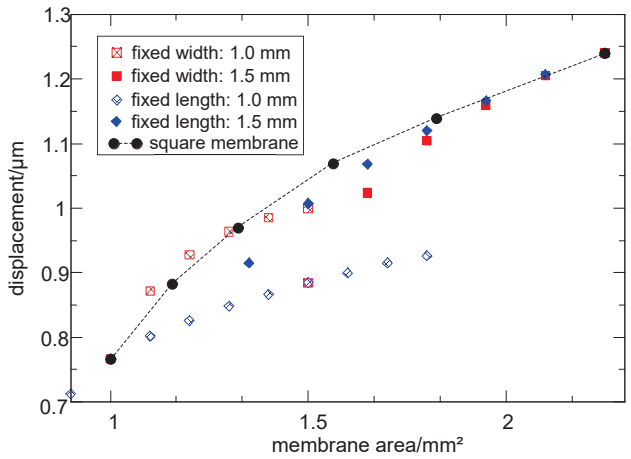

Figure 5: Maximal beam displacement as a function of the surface area of the membrane. Various geometrical constraints are denoted by different data point shapes and colors (see legend).

Nevertheless, due to fabrication tolerances and different resonance frequencies, the gap size is not the main parameter to tune sensitivity.

The main goal of this study is to increase the sensitivity of the sensor, which depends on the force exerted onto the beam, while keeping the resonance frequency constant. Since the sensor operates as a pressure gradient sensor, the force can be calculated by $F = \int \Delta p(x, y) dA$ with the sound pressure drop Δp between the front and back side of the beam and A the beam surface. Changing the surface area of the beam would modify the resonance frequency. Thus, sensitivity is most effectively tuned by varying the membrane geometry.
With this in mind, the membrane area is varied and two cases are considered: either the shape of the membrane is square, with the length and the width varied simultaneously, or a rectangular membrane is used, for which either the length or the width of the membrane is kept constant, while the other property is modified. As shown in Figure 5, enlarging the membrane area increases the pressure difference and therefore, the sensitivity. For large membrane areas, both cases (square and rectangular membrane) yield nearly the same results. However, for smaller membrane areas $< 1.7\,\mathrm{mm}^2$, changing the length (with a constant width) yields larger displacements than changing the width (with a constant length). The results for the square membrane are similar to the fixed width case. This should be an effect of the asymmetry of the beam, which is longer than it is wide. Due to this asymmetry, the extent of the margin around the beam is asymmetrical as well: With a square membrane, the margin is thinner at the free end of the beam along its length than at its sides. As a wider margin implies a larger Δp, this asymmetry ultimately shows in the displacement. Simply put, the displacement is limited by the thinnest margin around the beam.

Although the membrane can increase the sensitivity of the sensor, it will introduce artefacts like additional resonances and coupled beam-membrane modes if it is not mounted at all sides. To avoid this, the design additionally incorporates a mounting surrounding the membrane, realized by a 300–400 µm thick silicon body. Since the mounting will further influence the sound path, its influence on sensitivity was studied in the simulations. There, the mounting is implemented by 10 µm thick silicon walls of varying height (in z-direction), as shown in Figure 6.

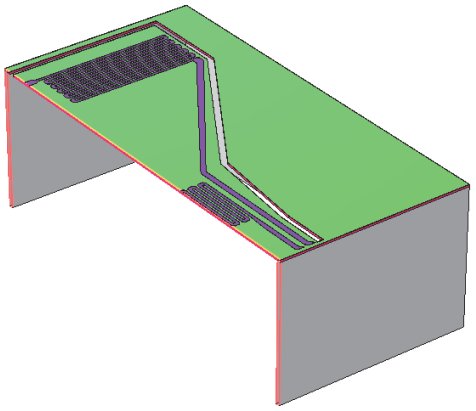

Figure 6: Three-dimensional view of the transducer design including a membrane and a mounting, with only the right half shown.

As can be seen in Figure 7, increasing the height of the mounting results in a decrease of the displacement for a membrane of size 1 mm × 1 mm, whereas for a larger membrane area of 1.5 mm × 1.5 mm an increase is observed. The latter is as expected from the increase in sound path around the structure and thus, the sound pressure difference on the beam. The decrease for the smaller membrane is probably caused by thermoviscous damping of the membrane movement where it is close to the mounting walls. Thus, to optimize sensitivity, large membrane areas with high mountings should be chosen if possible.

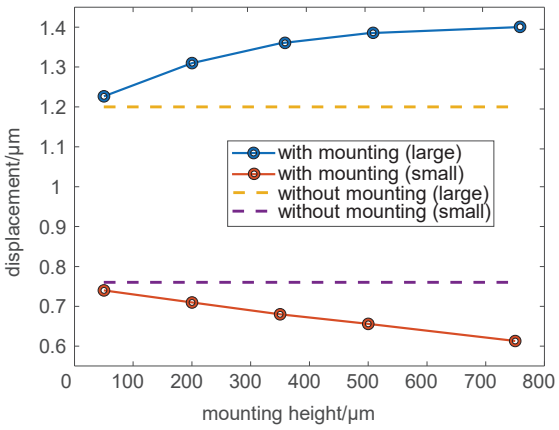

Figure 7: Maximum beam displacement as a function of mounting height. Different membrane areas and mounting setups are compared: 1.5 mm × 1.5 mm with mounting (blue), 1 mm × 1 mm with mounting (orange), 1.5 mm × 1.5 mm without mounting (dashed yellow), and 1 mm × 1 mm without mounting (dashed purple).

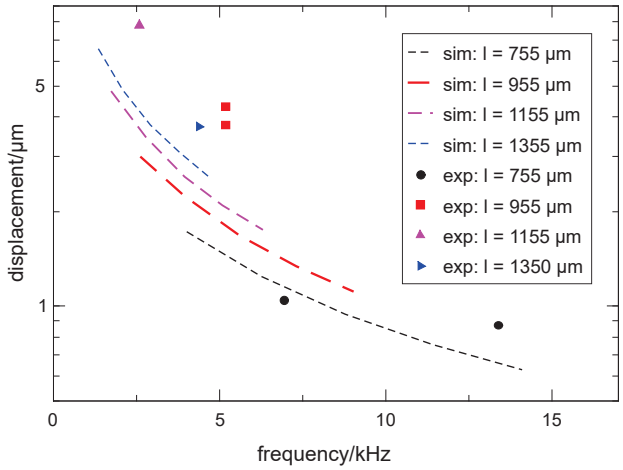

Figure 8: Comparison of experiment and simulation. The maximum beam displacement is plotted as a function of the resonance frequency for different lengths of the beam, surrounded by a 1.5 mm × 1.5 mm membrane and mounting. Changes in resonance frequency are obtained by varying the beam thickness. Dashed lines are results from the FEM simulations, symbols represent values from experiments.

Finally, we compared the simulation results with measurements of the sound response in an anechoic chamber combined with measurements by a vibrometer. Here, the measurements in the anechoic chamber were used to obtain the sensing voltage as a function of the sound pressure level, while the vibrometer measurements were used to calibrate the piezoresistive readout, i.e., correlate the sensing voltage amplitude with the maximum displacement of the free end of the beam.
The comparison is shown in Figure 8. As can be seen, in most cases the measured displacement was larger than the simulated one with a deviation up to 6 dB. One might immediately suspect a difference in the damping factors between experiment and simulation to cause this deviation, since the mechanical loss factors and the damping due to thermoviscous losses are not exactly known. However, the 3 dB bandwidths of the sensors determined from the experiment and the simulations are similar, showing a close agreement of the simulated damping with the experimental one. Therefore, another explanation seems more plausible: On some of the sensors in the experiment, the PCB for the readout extended partly into the beam area (on the side of the sound source). This obstacle may interfere with sound propagation, thus causing the difference between experiment and simulation results. This hypothesis will be tested in further studies.

Conclusions

In this article, we presented a study on a part of the geometrical design parameter space of a MEMS hair cell and the influence of design choices on the acoustic sensing properties. The goal was to be able to improve sensitivity without changing the resonance frequency. The study was based on FEM simulations, which were validated through measurements. Most importantly, we considered the effects of embedding the cantilever in a membrane of varying size. A sufficiently narrow gap between the cantilever and the membrane ensures mechanical decoupling but an acoustically sealed surface. Additionally, designs with a mounting of different height, around the edges of the membrane, were investigated. In summary, the addition of a membrane and a mounting is a viable method for increasing sensor sensitivity in the MEMS hair cells. However, mostly due to thermoviscous losses, some constraints regarding gap size, membrane area, and mounting height apply.
Pursuing other design variants, such as sealed enclosures, may offer specialized functionality (e.g., omnidirectional characteristic) or further improvements of the sensing properties in the future.

Acknowledgment

Funded by the Deutsche Forschungsgemeinschaft (German Research Foundation)-Project-ID 434434223 - SFB 1461 and the Carl-Zeiss-Stiftung in the project 'Memristive Materials for Neuromorphic Engineering (MemWerk)'.

References

[1] Papastratis, I.: Speech Recognition: a review of the different deep learning approaches, https: theaisummer.com (2021).

[2] Turpault, N. *et al.*: Sound Event Detection and Separation: A Benchmark on Desed Synthetic Soundscapes, IEEE International Conference on Acoustics, Speech and Signal Processing (ICASSP) 2021, doi: 10.1109/ICASSP39728.2021.9414789.

[3] Lenk, C. *et al.*: Neuromorphic sensing: a highly adaptive, nonlinear acoustic sensor, Nat. Elect. in publication (2023).

[4] Durstewitz, S., Lenk, C., Ziegler, M. : Bio-Inspired Acoustic Sensor with Gain Adaptation Enhancing Dynamic Range and Onset Detection, 2022 IEEE International Symposium on Circuits and Systems (ISCAS) (2022).

[5] Lenk, C. *et al.*: Bio-inspired, nonlinear and adaptive acoustic sensing – Study of sensor design – DAGA 2022 (2022).

[6] Rangelow, I. W. *et al.*: Review Article: Active scanning probes: A versatile toolkit for fast imaging and emerging nanofabrication, J. Vac. Sci. Technol. B 35 (6), 06G101 (2017).

[7] Ivanov, T.: Piezoresistive cantilevers with an integrated bimorph actuator, Thesis urn:nbn:de:hebis:34-1153 (2003).

[8] Küller, J., Zhyhkar, A., and Beer, D.: Sound Propagation in Microchannels, Fortschritte der Akustik – DAGA 2020 (2020).

[9] Stauffenberg, J. *et al.*: Determination of the mixing ratio of a flowing gas mixture with self-actuated microcantilevers, J. Sens. Sens. Syst. 9, 71-78 (2020).